



# 1 Importance of Ammonia Gas-Particle Conversion Ratio in Haze 2 Formation in the Rural Agricultural Environment

3 Jian Xu<sup>1</sup>, Jia Chen<sup>1</sup>, Na Zhao<sup>1</sup>, Guochen Wang<sup>1</sup>, Guangyuan Yu<sup>1</sup>, Hao Li<sup>1</sup>, Juntao Huo<sup>3</sup>, Yanfen  
4 Lin<sup>3</sup>, Qingyan Fu<sup>3</sup>, Hongyu Guo<sup>4</sup>, Congrui Deng<sup>1,2</sup>, Shan-Hu Lee<sup>5</sup>, Jianmin Chen<sup>1</sup>, Kan  
5 Huang<sup>1,2,6\*</sup>

6 <sup>1</sup>Shanghai Key Laboratory of Atmospheric Particle Pollution and Prevention (LAP<sup>3</sup>), Department of Environmental  
7 Science and Engineering, Fudan University, Shanghai 200433, People's Republic of China

8 <sup>2</sup>Institute of Eco-Chongming (IEC), 20 Cuiniao Road, Chenjiazhen, Shanghai 202162, People's Republic of China

9 <sup>3</sup>Shanghai Environmental Monitoring Center, Shanghai 200235, People's Republic of China

10 <sup>4</sup>Cooperative Institute for Research in Environmental Sciences and Department of Chemistry, University of  
11 Colorado, Boulder, Colorado 80309, United States

12 <sup>5</sup>Department of Atmospheric & Earth Science, University of Alabama in Huntsville, Huntsville, Alabama 35758,  
13 United States

14 <sup>6</sup>Institute of Atmospheric Sciences, Fudan University, Shanghai 200433, People's Republic of China

15 *Correspondence to:* Kan Huang (huangkan@fudan.edu.cn)

16 **Abstract.** Ammonia in the atmosphere is essential for the formation of fine particles that impact air quality and  
17 climate. Despite extensive prior research to disentangle the relationship between ammonia and haze pollution, the  
18 role of ammonia in haze formation in the high ammonia emitted regions is still not well understood. Aiming to  
19 better understand secondary inorganic aerosol (SNA) formation mechanisms under high ammonia conditions, one-  
20 year hourly measurement of water-soluble inorganic species (gas and particle) was conducted in a rural supersite in  
21 Shanghai. Exceedingly high levels of agricultural ammonia, constantly around 30  $\mu\text{g m}^{-3}$ , were observed. We find  
22 that ammonia gas-particle conversion ratio (ACR), as opposed to ammonia concentrations, plays a critical role in  
23 SNA formation during the haze period. By assessing the effects of various parameters, including temperature (T),  
24 aerosol water content (AWC), aerosol pH, and activity coefficient, it seems that AWC plays predominant regulating  
25 roles for ACR. We propose a self-amplifying feedback mechanism associated with ACR for the formation of SNA,  
26 which is consistent with diurnal variations of ACR, AWC, and SNA. Our results imply that reduction of ammonia  
27 emissions alone may not reduce SNA effectively at least in rural agricultural sites in China.

## 28 1 Introduction

29 Gas-phase ammonia ( $\text{NH}_3$ ) in the environment not only fuel the eutrophication and acidification of ecosystems, but  
30 also play key roles in atmospheric chemistry.  $\text{NH}_3$  has been known to promote new particle formation both in the  
31 initial homogeneous nucleation and subsequent growth (Ball et al., 1999; Zhang et al., 2011; Coffman and Hegg,  
32 1995; Kirkby et al., 2011). Prior studies suggest that the  $\text{SO}_2$  oxidation can be enhanced by the presence of  $\text{NH}_3$   
33 (Turšič et al., 2004; Wang et al., 2016; Benner et al., 1992). High levels of  $\text{NH}_3$  can also promote SOA formation (Na  
34 et al., 2007; Ortiz-Montalvo et al., 2013). As the main alkaline species in the atmosphere,  $\text{NH}_3$  are expected to affect  
35 the acidity of clouds (Wells et al., 1998), fine particles (Liu et al., 2017; Guo et al., 2017b), and wet deposition  
36 (ApSimon et al., 1987) by neutralizing acidic species. The neutralized ammonium ( $\text{NH}_4^+$ ) exclusively contribute to



37 aerosol hygroscopicity especially in hazy periods (Liu et al., 2017;Ye et al., 2011). Serving as efficient catalysts for  
38 aerosol aldol condensation, ammonium has also been proved to contribute to radiative forcing (Noziere et al.,  
39 2010;Park et al., 2014). Most importantly, ammonium is among the major secondary inorganic aerosols (i.e., sulfate  
40  $\text{SO}_4^{2-}$ , nitrate  $\text{NO}_3^-$ , and ammonium  $\text{NH}_4^+$ , denoted as SNA), which typically rivals the organics and can make up  
41 more than 50% of  $\text{PM}_{2.5}$  mass loadings (Wang et al., 2015a;Sun et al., 2014;Huang et al., 2014;Plautz, 2018;Schiferl  
42 et al., 2014). Despite the significant importance of SNA in hazy periods, its formation mechanism responsible,  
43 particularly the role of  $\text{NH}_3$ , remains highly controversial. Cheng et al. (2016) and Wang et al. (2016), for example,  
44 suggested that the near-neutral acidity, resulting from the  $\text{NH}_3$  rich atmosphere, is vital for SNA formation. While  
45 Liu et al. (2017) and Guo et al. (2017b) demonstrated that the close to neutral state is unlikely even under conditions  
46 of excess  $\text{NH}_3$ . These findings collectively imply that the fundamental role of  $\text{NH}_3$  in regulating aerosol acidity is  
47 still ambiguous, thus altering the SNA formation mechanism (Seinfeld and Pandis, 2012).

48  $\text{NH}_3$  emission sources include agricultural practices, on-road vehicles(Chang et al., 2016;Sun et al., 2016) and  
49 biomass burning (Lamarque et al., 2010;Paulot et al., 2017). Recent field measurements and modeling works reveal  
50 that agricultural practices (i.e., animal manure and fertilizer application) contribute to 80-90% of total  $\text{NH}_3$   
51 emissions in China (Zhang et al., 2018;Kang et al., 2016;Huang et al., 2011). Globally,  $\text{NH}_3$  emissions are projected  
52 to continue to rise along with increasing demand of chemical fertilizers due to the growing human population  
53 (Erismann et al., 2008;Stewart et al., 2005) and in part because limiting  $\text{NH}_3$  emissions has not been targeted a  
54 priority in most countries. For example, even though stringent mitigation targets have been set for  $\text{SO}_2$  and  $\text{NO}_x$  in  
55 China's 13th Five-Year Plan (2016-2020), slashing  $\text{NH}_3$  emissions is not yet a prime concern in China. The  
56 sustained increase of  $\text{NH}_3$  has been observed from the space (Warner et al., 2017) and reported to deflect the  
57 mitigation efforts of  $\text{SO}_2$  and  $\text{NO}_x$  emissions in East China (Fu et al., 2017).

58 Although agricultural  $\text{NH}_3$  emission has been the subject of extensive research, previous studies have focused on  
59 densely populated or urban areas, where  $\text{NH}_3$  was mostly "aged" and transformed to  $\text{NH}_4^+$  downwind (Chang et al.,  
60 2016). Varying in location and time, the typical mass concentrations of  $\text{NH}_3$  are on the order of several micrograms  
61 per cubic meter(Yao et al., 2006;Gong et al., 2013;Robarge et al., 2002;Chang et al., 2016;Phan et al., 2013), with  
62 extremely high levels up to more than  $20 \mu\text{g m}^{-3}$  in the rural area of North China Plain(Meng et al., 2018;Shen et al.,  
63 2011;Pan et al., 2018). Numerous studies highlighted the importance of  $\text{NH}_3$  emissions from agricultural areas  
64 (Meng et al., 2018;Shen et al., 2011;Robarge et al., 2002;Wang et al., 2013;Nowak et al., 2012;Zhang et al.,  
65 2017;Warner et al., 2017), but the gas-particle conversion of agricultural  $\text{NH}_3$  in rural regions and its subsequent  
66 impact on SNA formation, has scarcely been reported and remains poorly understood.

67 In this study, we provide observational constraints on the abnormally high agricultural  $\text{NH}_3$  emission at a rural site.  
68 We report our findings on the influence of  $\text{NH}_3$  gas-particle conversion ratio on SNA formation and discuss the  
69 decisive factors driving the  $\text{NH}_3$  gas-particle conversion ratio (ACR).



## 70 2 Methods

### 71 2.1 Observation site

72 Field measurements of gases and fine particles were conducted over the course of a year from March 2017 to  
73 February 2018 at the Dongtan Wetland Park (31°32' N, 121°58' E; altitude: 12 m a.s.l.), which is approximately 50  
74 km northeast of downtown Shanghai. The sampling site, illustrated in Figure 1, was located on the east side of the  
75 Chongming island, which is the largest eco-friendly island in China and the least developed district of Shanghai. The  
76 annual mean relative humidity (RH) is  $78\% \pm 19\%$  and the yearly average temperature (T) is  $16.3 \pm 9.9^\circ\text{C}$ . Although  
77 Chongming shares limited industrial and vehicle emissions compared to urban Shanghai, the level of fine particles  
78 on this island is slightly higher than the urban site (Figure S1). The overuse of nitrogen fertilizer has long been a  
79 large agricultural source of  $\text{NH}_3$  emissions in China (Fan et al., 2011), with an increasing use especially in East-  
80 Central China (Yang and Fang, 2015), where rice/wheat intercropping (similar to those in Chongming) was applied.  
81 Based on a 2011 agricultural  $\text{NH}_3$  emission inventory in Shanghai, Chongming has the largest nitrogen fertilizer  
82 consumption among all the districts in Shanghai (Fang et al., 2015). According to the Multi-resolution Emission  
83 Inventory for China (MEIC, [www.meicmodel.org](http://www.meicmodel.org)) in 2016, nearly 94% of  $\text{NH}_3$  in Chongming came from the  
84 agricultural sector, accounting for 14% of the total  $\text{NH}_3$  emissions in Shanghai. In comparison, Chongming  
85 contributes only 6% and 5% of the total  $\text{NO}_x$  and  $\text{SO}_2$  emissions in Shanghai, respectively (Table S1). With the most  
86 intensive agriculture and 34% of arable farmland area in Shanghai (Wen et al., 2011), atmospheric ammonium  
87 aerosols over the Chongming island are mostly of agricultural origin. Therefore, this site is ideal for investigating  
88 the role of agricultural emissions of  $\text{NH}_3$  in haze formation.

### 89 2.2 Measurements

90 Water-soluble samples of both gases ( $\text{NH}_3$ ,  $\text{SO}_2$ ,  $\text{HCl}$ ,  $\text{HNO}_2$ , and  $\text{HNO}_3$ ) and particles ( $\text{NH}_4^+$ ,  $\text{Na}^+$ ,  $\text{K}^+$ ,  $\text{Ca}^{2+}$ ,  $\text{Mg}^{2+}$ ,  
91  $\text{Cl}^-$ ,  $\text{NO}_3^-$ , and  $\text{SO}_4^{2-}$ ) were measured hourly using MARGA (Monitor for AeRosols and Gases in Air, ADI 2080,  
92 Metrohm Applikon B.V., Netherlands). Online sampling was conducted from March 2017 to February 2018  
93 following the description in Kong et al. (2014). Briefly, air was drawn into a  $\text{PM}_{2.5}$  cyclone inlet with a flow rate of 1  
94  $\text{m}^3 \text{h}^{-1}$  and passed through either a wet rotating denuder (gases) or a steam jet aerosol collector (aerosols).  
95 Subsequently, the aqueous samples were analyzed with ion chromatography. Meanwhile,  $\text{PM}_{2.5}$  and gaseous  
96 pollutants ( $\text{SO}_2$ ,  $\text{NO}_2$ ,  $\text{O}_3$ , and  $\text{CO}$ ) were monitored by co-located instruments. Mass loadings of  $\text{PM}_{2.5}$   
97 were determined by a Tapered Element Oscillating Microbalance coupled with Filter Dynamic Measurement System  
98 (TEOM 1405-F).  $\text{SO}_2$  mass concentrations were analyzed by Pulsed Fluorescence  $\text{SO}_2$  Analyzer (Thermo Fisher  
99 Scientific, Model 43i).  $\text{NO}_2$  mass concentrations were analyzed by Chemiluminescence  $\text{NO-NO}_2\text{-NO}_x$  Analyzer  
100 (Thermo Fisher Scientific, Model 42i).  $\text{O}_3$  mass concentrations were analyzed by UV Photometric Ozone Analyzer  
101 (Thermo Fisher Scientific, Model 49i).  $\text{CO}$  mass concentrations were analyzed by Gas Filter Correlation  $\text{CO}$   
102 Analyzer (Thermo Fisher Scientific, Model 48i). The QA/QC of these instruments were managed by professional  
103 staff in Shanghai Environmental Monitoring Center (SEMC) according to the Technical Guideline of Automatic  
104 Stations of Ambient Air Quality in Shanghai (HJ/T193-2005).



## 105 2.3 ISORROPIA-II modelling

106 The thermodynamic model ISORROPIA II (Fountoukis and Nenes, 2007) was used to predict the aerosol water  
107 content and pH. ISORROPIA was constrained in forward metastable mode by hourly averaged measurements of  $\text{Na}^+$ ,  
108  $\text{K}^+$ ,  $\text{Mg}^{2+}$ ,  $\text{Ca}^{2+}$ ,  $\text{SO}_4^{2-}$ ,  $\text{NH}_3$ ,  $\text{NH}_4^+$ ,  $\text{HNO}_3$ ,  $\text{NO}_3^-$ ,  $\text{HCl}$ , and  $\text{Cl}^-$ , along with RH and T. The molality based pH was a  
109 default output in the model. The model showed a good performance when predicting  $\text{NH}_3$ - $\text{NH}_4^+$  partitioning (Figure  
110 2).

## 111 3 Results and Discussion

### 112 3.1 $\text{NH}_3$ levels and its link to secondary inorganic aerosol

113 Figure 3 shows that the mean concentration of  $\text{NH}_3$  at Chongming (CM:  $17.0 \pm 4.2 \mu\text{g m}^{-3}$ ) is more than three times  
114 higher than an urban site in Shanghai (PD:  $2.5 \pm 0.9 \mu\text{g m}^{-3}$ ) and a representative regional transport region (DL:  $4.6$   
115  $\pm 2.0 \mu\text{g m}^{-3}$ ) in the Yangtze River Delta. The level of  $\text{NH}_3$  at Chongming is even close to that observed inside a  
116 typical dairy farm (JS:  $19.4 \pm 12.6 \mu\text{g m}^{-3}$ ), which is dominated by livestock emissions. Thus, it is interesting to  
117 investigate how the formation of secondary inorganic aerosols is impacted by this abnormally high level of  $\text{NH}_3$ .  
118 Figure 4 indicates the response of SNA (sulfate, nitrate, and ammonium) mass concentrations to  $\text{NH}_3$  is nonlinear.  
119 Higher  $\text{NH}_3$  sometimes correspond to even lower SNA mass concentrations. Statistically, the average SNA  
120 concentration in each bin of  $\text{NH}_3$  doesn't show significant difference. This is at odds with the traditional view that  
121 higher concentrations of precursors usually result in elevated inorganic aerosols (Nowak et al., 2010). Although the  
122 abundance of SNA is related to the alkaline gaseous precursor (e.g.,  $\text{NH}_3$ ), the ambient condition (e.g., RH and T),  
123 and acid precursors (i.e.,  $\text{SO}_2$  and  $\text{NO}_x$ ) whether favor the conversion of precursors into particles or not is equally  
124 important, if not higher. For example, the urban areas show higher SNA levels than the rural region while lower  
125  $\text{NH}_3$  mixing ratio was observed (Wu et al., 2016; Wang et al., 2015b). Previous field measurements suggest that rural  
126  $\text{NH}_4^+$  levels are more sensitive to acidic gases than to the  $\text{NH}_3$  availability (Shen et al., 2011; Robarge et al., 2002).  
127 Therefore, the level of  $\text{NH}_3$  concentration is not the determining factor for the formation of secondary inorganic  
128 aerosols.

### 129 3.2 The role of ammonia gas-particle conversion ratio

130 In this regard, we further investigate the relationship between the ammonia gas-particle conversion ratio (ACR,  
131 defined as the molar ratio between particle phase ammonia ( $\text{NH}_4^+$ ) and total ammonia ( $\text{NH}_x = \text{NH}_3 + \text{NH}_4^+$ )) and SNA  
132 during the haze period. The haze period is defined as hourly averaged  $\text{PM}_{2.5}$  mass loadings higher than  $75 \mu\text{g m}^{-3}$ .  
133 As shown in Figure 5, it is obvious that SNA in  $\text{PM}_{2.5}$  is almost linearly correlated with ACR. Higher ACR results in  
134 higher SNA concentrations. In addition, under the same ACR conditions, higher  $\text{NH}_3$  promotes stronger formation  
135 of SNA. Thus,  $\text{NH}_3$  and ACR collectively determine the haze formation potential. The level of  $\text{NH}_3$  can be regarded  
136 as a proxy of  $\text{NH}_3$  emission intensity, which is source dependent. As for ACR, it represents the relative abundance  
137 of gaseous  $\text{NH}_3$  and particulate ammonium. The shift between the two phases is controlled by various factors such  
138 as the ambient environmental conditions. Previous study shows that elevated RH and acidic gas levels favor the shift



139 of  $\text{NH}_3$  towards the particulate phase at an urban site, thereby a lower  $[\text{NH}_3]:[\text{NH}_4^+]$  ratio was observed (Wei et al.,  
140 2015). In this study, it is also observed that higher ACR values coincide with heightened RH,  $\text{SO}_2$ , and  $\text{NO}_x$ .

141 Based on the above results, elucidation of the driving factors determining ACR is of great importance to explore the  
142 formation mechanism of haze. Theoretically, ACR is determined by  $\text{NH}_3$ ,  $\text{NH}_4^+$ , and the equilibrium between  $\text{NH}_3$   
143 and  $\text{NH}_4^+$ . Assuming  $\text{NH}_3$  and  $\text{NH}_4^+$  are in thermodynamic equilibrium, the following equation can be obtained.



145 The equilibrium constant  $H_{\text{NH}_3}^*$  is equal to the Henry's constant of  $\text{NH}_3$  divided by the acid dissociation constant for  
146  $\text{NH}_4^+$  (Clegg et al., 1998b).  $H_{\text{NH}_3}^*$  is calculated by the following equation:

$$147 \quad \ln(H_{\text{NH}_3}^*) = 25.393 - 10373.6(1/T_r - 1/T) + 4.131(T_r/T - (1 + \ln(T_r/T))) \quad (\text{Eq. 1})$$

148 here,  $T_r$  is the reference temperature of 298.15 K. ACR can be analytically calculated as detailed in Guo et  
149 al.(2017a) via the following equation:

$$150 \quad \text{ACR} = \frac{[\text{NH}_4^+]}{[\text{NH}_x]} \cong \frac{\frac{\gamma_{\text{H}^+} 10^{-\text{pH}}}{\gamma_{\text{NH}_4^+}} H_{\text{NH}_3}^* W_i RT \times 0.987 \times 10^{-14}}{1 + \frac{\gamma_{\text{H}^+} 10^{-\text{pH}}}{\gamma_{\text{NH}_4^+}} H_{\text{NH}_3}^* W_i RT \times 0.987 \times 10^{-14}} \quad (\text{Eq. 2})$$

151 here,  $[\text{NH}_4^+]$  is the molar concentration of  $\text{NH}_4^+$  (mole  $\text{m}^{-3}$ ).  $\gamma$  is the activity coefficient, which is extracted from the  
152 E-AIM IV model (Clegg et al., 1998a) to account for the non-ideality solution effect.  $H_{\text{NH}_3}^*$  ( $\text{atm}^{-1}$ ) represents the  
153 molality-based equilibrium constant, which is T dependent and can be determined using equation (12) in Clegg et  
154 al.(1998b).  $W_i$  ( $\mu\text{g m}^{-3}$ ) is the aerosol water content predicted by ISORROPIA-II. R (J/mole/K) is the universal gas  
155 constant. T (K) is ambient temperature and  $0.987 \times 10^{-14}$  is the conversion multiplication factors from atm and  $\mu\text{g}$  to  
156 SI units.

157 In Figure 6, ACR curve (The “S” shape curve, referred to as “S Curve” hereafter) is plotted against pH based on the  
158 average T (10°C), AWC (100  $\mu\text{g m}^{-3}$ ), and  $\frac{\gamma_{\text{H}^+}}{\gamma_{\text{NH}_4^+}}$  (2.4) during the haze period. Observation-based ACR as a function

159 of pH with varying T and AWC is also shown. Clearly, the observational ACR data points are relatively well  
160 constrained by the theoretical equation, suggestive of reasonable judgement that ACR is controlled by T, AWC, pH,  
161 and  $\frac{\gamma_{\text{H}^+}}{\gamma_{\text{NH}_4^+}}$ . Under the condition of average pH ( $4.6 \pm 0.3$ ) during the winter haze period, the “S curve” derives ACR

162 of 0.2, around half of the average measured ACR ( $0.4 \pm 0.1$ ). Regional and long-range transport of aerosol pollutants  
163 from northern China during the cold season (Xu et al., 2018) may have increased  $\text{NH}_4^+$ , yet  $\text{NH}_3$  remains little  
164 unaffected because of its limited transport distance (Asman et al., 1998). The transport effect cannot be predicted by  
165 the theoretical equation and this should partly explain the divergence between the calculated and observed ACR.  
166 Earlier works have also observed higher particle phase fraction than the Henry's law constants predicted for water  
167 soluble aerosol components (Arellanes et al., 2006; Hennigan et al., 2008; Shen et al., 2018). Another possible factor  
168 contributing to the underestimation of ACR is the unaccounted effect from organic species, whose role in driving the  
169 SNA formation is thought to be significant (Silvern et al., 2017). The organics have been found to account for 35%  
170 of AWC in the southeast USA (Guo et al., 2015), thus ACR would be enhanced by including organic aerosol. To  
171 quantitatively determine which parameter dominates the ACR, the impact on ACR from individual variable (i.e. T,



172 AWC, pH, and  $\frac{Y_{H^+}}{Y_{NH_4^+}}$  during the haze period in winter is assessed (Figure 7). From a theoretical perspective, the  
173 decrease of pH and T, and increase of AWC and  $\frac{Y_{H^+}}{Y_{NH_4^+}}$  would raise ACR. For instance, in summertime, the lower  
174 ACR (Figure 4) are mainly due to higher T that shift the equilibrium to the gas phase, thus higher  $NH_3$  ( $40 \pm 8 \mu g m^{-3}$ )  
175 while lower  $NH_4^+$  was observed. Likewise, in wintertime, the lower T facilitates the residence of  $NH_4^+$  in the  
176 particle phase than the gas phase ( $NH_3$ :  $20 \pm 4 \mu g m^{-3}$ ), resulting in higher ACR.  
177 On the basis of “S curve” (Figure 7), each 0.1 unit change of ACR can be caused by approximate  $5 \text{ }^\circ C$ ,  $75 \mu g m^{-3}$ ,  
178 0.3, and 2 units change of T, AWC, pH, and  $\frac{Y_{H^+}}{Y_{NH_4^+}}$ , respectively. Actually, T, pH, and  $\frac{Y_{H^+}}{Y_{NH_4^+}}$  are within a relatively  
179 narrow range during the winter haze period (Table 1), suggesting the variation of these parameters shouldn't result  
180 in the significant change of ACR. On the contrary, AWC fluctuates greatly during the study period (Table 1).  
181 Therefore, AWC should be the key factor regulating ACR. It is well established that AWC is a function of RH and  
182 atmospheric aerosol compositions (Pilinis et al., 1989; Wu et al., 2018; Nguyen et al., 2016; Hodas et al., 2014). AWC  
183 has been known to promote secondary aerosol formation by providing aqueous medium for uptake of reactive gases,  
184 gas to particle partitioning, and the subsequent chemical processing (McNeill, 2015; McNeill et al., 2012; Tan et al.,  
185 2009; Xu et al., 2017b).  
186 The winter haze pH in this study were  $\sim 3$  units higher than that of the southeastern United States summer campaign  
187 (Nah et al., 2018; Guo et al., 2015; Guo et al., 2017a; Xu et al., 2017a), but close to that of 3.7 in rural Europe (Guo et  
188 al., 2018) and 4.2 in North China Plain (Liu et al., 2017), where  $NH_3$ -rich conditions are prevalent. AWC may act as  
189 the major factor, because greater AWC dilute the  $[H^+]$  and raise the pH. The AWC during the haze period ( $82 \pm 105$   
190  $\mu g m^{-3}$ ) were much higher than those during the non-haze period ( $32 \pm 41 \mu g m^{-3}$ ).

### 191 3.3 A possible self-amplifying feedback mechanism

192 Given that AWC is a function of RH and SNA, a conceptual model of how AWC control ACR can be illustrated by  
193 a self-amplifying feedback loop (Figure 8). Formation of SNA is initiated by gas-particle conversion of  $NH_3$ . Under  
194 certain meteorological conditions such as high RH and shallow planetary boundary layer, SNA is subject to uptake  
195 moisture and result in the increases of AWC. Based on the discussions above, the increase of AWC would further  
196 raise ACR, leading to more efficient transformation of  $NH_3$  as SNA.  
197 Figure 9 shows the yearly average diurnal variation of ACR, AWC, SNA along with T and RH. Apparently, SNA  
198 tracked well with ACR and AWC, especially over nighttime. The not well-correlated track between SNA and AWC  
199 and ACR during the daytime (8:00-16:00) can be ascribed to the photochemical reactions that lead to SNA  
200 formation. The good correlation between SNA and AWC and ACR demonstrated in figure 9 support the proposed  
201 self-amplifying feedback loop in SNA formation.

### 202 4 Conclusion

203 Our results demonstrate that ACR, rather than  $NH_3$  concentrations, plays a critical role in driving haze formation in  
204 the agricultural  $NH_3$  emitted regions. Based on the “S curve” calculation, we have unraveled that AWC is the major



205 factor controlling ACR. Upon analyzing the cross-correlations between AWC, ACR and SNA, we proposed a self-  
206 amplifying feedback mechanism of SNA formation that associated with AWC and ACR. This positive feedback  
207 cycle is likely to occur in other rural regions, where high agricultural  $\text{NH}_3$  emissions are prevalent.

208 We have shown that high  $\text{NH}_3$  concentrations may not necessarily lead to strong SNA formation, particularly in the  
209 agriculture intensive areas, e.g. the North China Plain (NCP) and the extensive farming lands in Eastern China  
210 where the high  $\text{NH}_3$  levels are still unregulated and increasing (Meng et al., 2018; Warner et al., 2017). Although Liu  
211 et al. (2019) have predicted that  $\text{PM}_{2.5}$  can be slashed by 11-17% when 50% reduction in  $\text{NH}_3$  from the agricultural  
212 sector and 15% mitigation of  $\text{NO}_x$  and  $\text{SO}_2$  emissions was achieved, a recent study has demonstrated that only when  
213 aerosol pH drops below 3.0, the  $\text{NH}_3$  reduction would have expected mitigation effects (Guo et al., 2018). The  
214 winter haze pH ( $4.6 \pm 0.3$ ) in this study was mostly between 4-5. Our results thus imply that  $\text{NH}_3$  only may not be an  
215 effective solution to tackle air pollution in these regions.

216 ***Data availability.***

217 The data presented in this paper are available upon request from the corresponding author ([huangkan@fudan.edu.cn](mailto:huangkan@fudan.edu.cn)).

218 ***Author contributions.***

219 JX and KH conceived the study. JX, JC, and KH performed data analysis and wrote the paper. All authors  
220 contributed to the review of the manuscript.

221 ***Competing interests.***

222 The authors declare that they have no conflict of interest.

223 ***Acknowledgements***

224 The authors acknowledge support of the National Science Foundation of China (No. 91644105), the National Key  
225 R&D Program of China (2018YFC0213105), and the Natural Science Foundation of Shanghai (19ZR1421100). Jian  
226 Xu acknowledge project funded by China Postdoctoral Science Foundation (2019M651365).



## References

- 230 ApSimon, H. M., Kruse, M., and Bell, J. N. B.: Ammonia emissions and their role in acid deposition, *Atmospheric Environment*, 21, 1939-1946, 10.1016/0004-6981(87)90154-5, 1987.
- Arellanes, C., Paulson, S. E., Fine, P. M., and Sioutas, C.: Exceeding of Henry's Law by Hydrogen Peroxide Associated with Urban Aerosols, *Environmental Science & Technology*, 40, 4859-4866, 10.1021/es0513786, 2006.
- Asman, W. A. H., Sutton, M. A., and Schjørring, J. K.: Ammonia: emission, atmospheric transport and deposition, *New Phytologist*, 139, 27-48, 10.1046/j.1469-8137.1998.00180.x, 1998.
- 235 Ball, S. M., Hanson, D. R., Eisele, F. L., and McMurry, P. H.: Laboratory studies of particle nucleation: Initial results for H<sub>2</sub>SO<sub>4</sub>, H<sub>2</sub>O, and NH<sub>3</sub> vapors, *Journal of Geophysical Research: Atmospheres*, 104, 23709-23718, doi:10.1029/1999JD900411, 1999.
- Benner, W. H., Ogorevc, B., and Novakov, T.: Oxidation of SO<sub>2</sub> in thin water films containing NH<sub>3</sub>, *Atmospheric Environment. Part A. General Topics*, 26, 1713-1723, 10.1016/0960-1686(92)90069-W, 1992.
- 240 Chang, Y., Zou, Z., Deng, C., Huang, K., Collett, J. L., Lin, J., and Zhuang, G.: The importance of vehicle emissions as a source of atmospheric ammonia in the megacity of Shanghai, *Atmospheric Chemistry and Physics*, 16, 3577-3594, 10.5194/acp-16-3577-2016, 2016.
- Cheng, Y., Zheng, G., Wei, C., Mu, Q., Zheng, B., Wang, Z., Gao, M., Zhang, Q., He, K., Carmichael, G., Pöschl, U., and Su, H.: Reactive nitrogen chemistry in aerosol water as a source of sulfate during haze events in China, *Science Advances*, 2, e1601530, 10.1126/sciadv.1601530, 2016.
- 245 Clegg, S. L., Brimblecombe, P., and Wexler, A. S.: Thermodynamic model of the system H<sup>+</sup>-NH<sub>4</sub><sup>+</sup>-Na<sup>+</sup>-SO<sub>4</sub><sup>2-</sup>-NO<sub>3</sub><sup>-</sup>-Cl<sup>-</sup>-H<sub>2</sub>O at 298.15 K, *The Journal of Physical Chemistry A*, 102, 2155-2171, 10.1021/jp973043j, 1998a.
- Clegg, S. L., Brimblecombe, P., and Wexler, A. S.: Thermodynamic Model of the System H<sup>+</sup>-NH<sub>4</sub><sup>+</sup>-SO<sub>4</sub><sup>2-</sup>-NO<sub>3</sub><sup>-</sup>-H<sub>2</sub>O at Tropospheric Temperatures, *The Journal of Physical Chemistry A*, 102, 2137-2154, 10.1021/jp973042r, 1998b.
- Coffman, D. J., and Hegg, D. A.: A preliminary study of the effect of ammonia on particle nucleation in the marine boundary layer, *Journal of Geophysical Research: Atmospheres*, 100, 7147-7160, 10.1029/94JD03253, 1995.
- 250 Erisman, J. W., Sutton, M. A., Galloway, J., Klimont, Z., and Winiwarter, W.: How a century of ammonia synthesis changed the world, *Nature Geoscience*, 1, 636-639, 10.1038/ngeo325, 2008.
- Fan, M., Shen, J., Yuan, L., Jiang, R., Chen, X., Davies, W. J., and Zhang, F.: Improving crop productivity and resource use efficiency to ensure food security and environmental quality in China, *Journal of Experimental Botany*, 63, 13-24, 10.1093/jxb/err248, 2011.
- Fang, X., Shen, G., Xu, C., Qian, X., Li, J., Zhao, Z., Yu, S., and Zhu, C.: Agricultural ammonia emission inventory and its distribution characteristics in Shanghai, *Acta Agriculturae Zhejiangensis*, 27, 2177-2185 [In Chinese], 2015.
- 255 Fountoukis, C., and Nenes, A.: ISORROPIA II: a computationally efficient thermodynamic equilibrium model for K<sup>+</sup>-Ca<sup>2+</sup>-Mg<sup>2+</sup>-NH<sub>4</sub><sup>+</sup>-Na<sup>+</sup>-SO<sub>4</sub><sup>2-</sup>-NO<sub>3</sub><sup>-</sup>-Cl<sup>-</sup>-H<sub>2</sub>O aerosols, *Atmos. Chem. Phys.*, 7, 4639-4659, 10.5194/acp-7-4639-2007, 2007.
- Fu, X., Wang, S., Xing, J., Zhang, X., Wang, T., and Hao, J.: Increasing Ammonia Concentrations Reduce the Effectiveness of Particle Pollution Control Achieved via SO<sub>2</sub> and NO<sub>x</sub> Emissions Reduction in East China, *Environmental Science & Technology Letters*, 4, 221-227, 10.1021/acs.estlett.7b00143, 2017.
- 260 Gong, L., Lewicki, R., Griffin, R. J., Tittel, F. K., Lonsdale, C. R., Stevens, R. G., Pierce, J. R., Malloy, Q. G. J., Travis, S. A., Bobmanuel, L. M., Lefer, B. L., and Flynn, J. H.: Role of atmospheric ammonia in particulate matter formation in Houston during summertime, *Atmospheric Environment*, 77, 893-900, 10.1016/j.atmosenv.2013.04.079, 2013.
- Guo, H., Xu, L., Bougiatioti, A., Cerully, K. M., Capps, S. L., Hite Jr, J. R., Carlton, A. G., Lee, S. H., Bergin, M. H., Ng, N. L., Nenes, A., and Weber, R. J.: Fine-particle water and pH in the southeastern United States, *Atmos. Chem. Phys.*, 15, 5211-5228, 10.5194/acp-15-5211-2015, 2015.
- 265 Guo, H., Liu, J., Froyd, K. D., Roberts, J. M., Veres, P. R., Hayes, P. L., Jimenez, J. L., Nenes, A., and Weber, R. J.: Fine particle pH and gas-particle phase partitioning of inorganic species in Pasadena, California, during the 2010 CalNex campaign, *Atmos. Chem. Phys.*, 17, 5703-5719, 10.5194/acp-17-5703-2017, 2017a.
- 270 Guo, H., Weber, R. J., and Nenes, A.: High levels of ammonia do not raise fine particle pH sufficiently to yield nitrogen oxide-dominated sulfate production, *Scientific Reports*, 7, 12109, 10.1038/s41598-017-11704-0, 2017b.
- Guo, H., Otjes, R., Schlag, P., Kiendler-Scharr, A., Nenes, A., and Weber, R. J.: Effectiveness of ammonia reduction on control of fine particle nitrate, *Atmos. Chem. Phys.*, 18, 12241-12256, 10.5194/acp-18-12241-2018, 2018.
- 275 Hennigan, C. J., Bergin, M. H., Dibb, J. E., and Weber, R. J.: Enhanced secondary organic aerosol formation due to water uptake by fine particles, *Geophysical Research Letters*, 35, L18801, 10.1029/2008GL035046, 2008.
- Hodas, N., Sullivan, A. P., Skog, K., Keutsch, F. N., Collett, J. L., Decesari, S., Facchini, M. C., Carlton, A. G., Laaksonen, A., and Turpin, B. J.: Aerosol Liquid Water Driven by Anthropogenic Nitrate: Implications for Lifetimes of Water-Soluble Organic Gases and Potential for Secondary Organic Aerosol Formation, *Environmental Science & Technology*, 48, 11127-11136, 10.1021/es5025096, 2014.





- 280 Huang, C., Chen, C. H., Li, L., Cheng, Z., Wang, H. L., Huang, H. Y., Streets, D. G., Wang, Y. J., Zhang, G. F., and Chen, Y. R.: Emission inventory of anthropogenic air pollutants and VOC species in the Yangtze River Delta region, China, *Atmos. Chem. Phys.*, 11, 4105-4120, 10.5194/acp-11-4105-2011, 2011.
- 285 Huang, R.-J., Zhang, Y., Bozzetti, C., Ho, K.-F., Cao, J.-J., Han, Y., Daellenbach, K. R., Slowik, J. G., Platt, S. M., Canonaco, F., Zotter, P., Wolf, R., Pieber, S. M., Brun, E. A., Crippa, M., Ciarelli, G., Piazzalunga, A., Schwikowski, M., Abbaszade, G., Schnelle-Kreis, J., Zimmermann, R., An, Z., Szidat, S., Baltensperger, U., Haddad, I. E., and Prevot, A. S. H.: High secondary aerosol contribution to particulate pollution during haze events in China, *Nature*, 514, 218-222, 10.1038/nature13774, 2014.
- Kang, Y., Liu, M., Song, Y., Huang, X., Yao, H., Cai, X., Zhang, H., Kang, L., Liu, X., Yan, X., He, H., Zhang, Q., Shao, M., and Zhu, T.: High-resolution ammonia emissions inventories in China from 1980 to 2012, *Atmos. Chem. Phys.*, 16, 2043-2058, 10.5194/acp-16-2043-2016, 2016.
- 290 Kirkby, J., Curtius, J., Almeida, J., Dunne, E., Duplissy, J., Ehrhart, S., Franchin, A., Gagné, S., Ickes, L., Kürten, A., Kupc, A., Metzger, A., Riccobono, F., Rondo, L., Schobesberger, S., Tsagkogeorgas, G., Wimmer, D., Amorim, A., Bianchi, F., Breitenlechner, M., David, A., Dommen, J., Downard, A., Ehn, M., Flagan, R. C., Haider, S., Hansel, A., Hauser, D., Jud, W., Junninen, H., Kreissl, F., Kvashin, A., Laaksonen, A., Lehtipalo, K., Lima, J., Lovejoy, E. R., Makhmutov, V., Mathot, S., Mikkilä, J., Minginette, P., Mogo, S., Nieminen, T., Onnela, A., Pereira, P., Petäjä, T., Schnitzhofer, R., Seinfeld, J. H., Sipilä, M., Stozhkov, Y., Stratmann, F., Tomé, A., Vanhanen, J., Viisanen, Y., Virtala, A., Wagner, P. E., Walther, H., Weingartner, E., Wex, H., Winkler, P. M., Carslaw, K. S., Worsnop, D. R., Baltensperger, U., and Kulmala, M.: Role of sulphuric acid, ammonia and galactic cosmic rays in atmospheric aerosol nucleation, *Nature*, 476, 429, 10.1038/nature10343, 2011.
- 295 Kong, L., Yang, Y., Zhang, S., Zhao, X., Du, H., Fu, H., Zhang, S., Cheng, T., Yang, X., and Chen, J.: Observations of linear dependence between sulfate and nitrate in atmospheric particles, *Journal of Geophysical Research: Atmospheres*, 119, 341-361, 10.1002/2013JD020222, 2014.
- 300 Lamarque, J. F., Bond, T. C., Eyring, V., Granier, C., Heil, A., Klimont, Z., Lee, D., Liou, S. C., Mieville, A., Owen, B., Schultz, M. G., Shindell, D., Smith, S. J., Stehfest, E., Van Aardenne, J., Cooper, O. R., Kainuma, M., Mahowald, N., McConnell, J. R., Naik, V., Riahi, K., and van Vuuren, D. P.: Historical (1850–2000) gridded anthropogenic and biomass burning emissions of reactive gases and aerosols: methodology and application, *Atmos. Chem. Phys.*, 10, 7017-7039, 10.5194/acp-10-7017-2010, 2010.
- 305 Liu, M., Song, Y., Zhou, T., Xu, Z., Yan, C., Zheng, M., Wu, Z., Hu, M., Wu, Y., and Zhu, T.: Fine particle pH during severe haze episodes in northern China, *Geophysical Research Letters*, 44, 5213-5221, 10.1002/2017GL073210, 2017.
- Liu, M., Huang, X., Song, Y., Tang, J., Cao, J., Zhang, X., Zhang, Q., Wang, S., Xu, T., Kang, L., Cai, X., Zhang, H., Yang, F., Wang, H., Yu, J. Z., Lau, A. K. H., He, L., Huang, X., Duan, L., Ding, A., Xue, L., Gao, J., Liu, B., and Zhu, T.: Ammonia emission control in China would mitigate haze pollution and nitrogen deposition, but worsen acid rain, *Proceedings of the National Academy of Sciences*, 116, 7760-7765, 10.1073/pnas.1814880116, 2019.
- 310 McNeill, V. F., Woo, J. L., Kim, D. D., Schwieter, A. N., Wannell, N. J., Sumner, A. J., and Barakat, J. M.: Aqueous-Phase Secondary Organic Aerosol and Organosulfate Formation in Atmospheric Aerosols: A Modeling Study, *Environmental Science & Technology*, 46, 8075-8081, 10.1021/es3002986, 2012.
- McNeill, V. F.: Aqueous Organic Chemistry in the Atmosphere: Sources and Chemical Processing of Organic Aerosols, *Environmental Science & Technology*, 49, 1237-1244, 10.1021/es5043707, 2015.
- 315 Meng, Z., Xu, X., Lin, W., Ge, B., Xie, Y., Song, B., Jia, S., Zhang, R., Peng, W., Wang, Y., Cheng, H., Yang, W., and Zhao, H.: Role of ambient ammonia in particulate ammonium formation at a rural site in the North China Plain, *Atmos. Chem. Phys.*, 18, 167-184, 10.5194/acp-18-167-2018, 2018.
- Na, K., Song, C., Switzer, C., and Cocker, D. R.: Effect of Ammonia on Secondary Organic Aerosol Formation from  $\alpha$ -Pinene Ozonolysis in Dry and Humid Conditions, *Environmental Science & Technology*, 41, 6096-6102, 10.1021/es061956y, 2007.
- 320 Nah, T., Guo, H., Sullivan, A. P., Chen, Y., Tanner, D. J., Nenes, A., Russell, A., Ng, N. L., Huey, L. G., and Weber, R. J.: Characterization of aerosol composition, aerosol acidity, and organic acid partitioning at an agriculturally intensive rural southeastern US site, *Atmos. Chem. Phys.*, 18, 11471-11491, 10.5194/acp-18-11471-2018, 2018.
- Nguyen, T. K. V., Zhang, Q., Jimenez, J. L., Pike, M., and Carlton, A. G.: Liquid Water: Ubiquitous Contributor to Aerosol Mass, *Environmental Science & Technology Letters*, 3, 257-263, 10.1021/acs.estlett.6b00167, 2016.
- 325 Nowak, J. B., Neuman, J. A., Bahreini, R., Brock, C. A., Middlebrook, A. M., Wollny, A. G., Holloway, J. S., Peischl, J., Ryerson, T. B., and Fehsenfeld, F. C.: Airborne observations of ammonia and ammonium nitrate formation over Houston, Texas, *Journal of Geophysical Research: Atmospheres*, 115, D22304, 10.1029/2010JD014195, 2010.
- Nowak, J. B., Neuman, J. A., Bahreini, R., Middlebrook, A. M., Holloway, J. S., McKeen, S. A., Parrish, D. D., Ryerson, T. B., and Trainer, M.: Ammonia sources in the California South Coast Air Basin and their impact on ammonium nitrate formation, *Geophysical Research Letters*, 39, L07804, 10.1029/2012GL051197, 2012.
- 330 Nozière, B., Dziedzic, P., and Cordova, A.: Inorganic ammonium salts and carbonate salts are efficient catalysts for aldol condensation in atmospheric aerosols, *Physical Chemistry Chemical Physics*, 12, 3864-3872, 10.1039/B924443C, 2010.



- Ortiz-Montalvo, D. L., Häkkinen, S. A. K., Schwier, A. N., Lim, Y. B., McNeill, V. F., and Turpin, B. J.: Ammonium Addition (and Aerosol pH) Has a Dramatic Impact on the Volatility and Yield of Glyoxal Secondary Organic Aerosol, *Environmental Science & Technology*, 48, 255-262, 10.1021/es4035667, 2013.
- 335 Pan, Y., Tian, S., Zhao, Y., Zhang, L., Zhu, X., Gao, J., Huang, W., Zhou, Y., Song, Y., Zhang, Q., and Wang, Y.: Identifying Ammonia Hotspots in China Using a National Observation Network, *Environmental Science & Technology*, 52, 3926-3934, 10.1021/acs.est.7b05235, 2018.
- 340 Park, R. S., Lee, S., Shin, S. K., and Song, C. H.: Contribution of ammonium nitrate to aerosol optical depth and direct radiative forcing by aerosols over East Asia, *Atmos. Chem. Phys.*, 14, 2185-2201, 10.5194/acp-14-2185-2014, 2014.
- Paulot, F., Paynter, D., Ginoux, P., Naik, V., Whitburn, S., Van Damme, M., Clarisse, L., Coheur, P. F., and Horowitz, L. W.: Gas-aerosol partitioning of ammonia in biomass burning plumes: Implications for the interpretation of spaceborne observations of ammonia and the radiative forcing of ammonium nitrate, *Geophysical Research Letters*, 44, 8084-8093, 10.1002/2017GL074215, 2017.
- 345 Phan, N.-T., Kim, K.-H., Shon, Z.-H., Jeon, E.-C., Jung, K., and Kim, N.-J.: Analysis of ammonia variation in the urban atmosphere, *Atmospheric Environment*, 65, 177-185, 10.1016/j.atmosenv.2012.10.049, 2013.
- Pilinis, C., Seinfeld, J. H., and Grosjean, D.: Water content of atmospheric aerosols, *Atmospheric Environment*, 23, 1601-1606, 10.1016/0004-6981(89)90419-8, 1989.
- Plautz, J.: Piercing the haze, *Science*, 361, 1060, 2018.
- 350 Robarge, W. P., Walker, J. T., McCulloch, R. B., and Murray, G.: Atmospheric concentrations of ammonia and ammonium at an agricultural site in the southeast United States, *Atmospheric Environment*, 36, 1661-1674, 10.1016/S1352-2310(02)00171-1, 2002.
- Schiferl, L. D., Heald, C. L., Nowak, J. B., Holloway, J. S., Neuman, J. A., Bahreini, R., Pollack, I. B., Ryerson, T. B., Wiedinmyer, C., and Murphy, J. G.: An investigation of ammonia and inorganic particulate matter in California during the CalNex campaign, *Journal of Geophysical Research: Atmospheres*, 119, 1883-1902, 10.1002/2013JD020765, 2014.
- 355 Seinfeld, J. H., and Pandis, S. N.: *Atmospheric chemistry and physics: from air pollution to climate change*, Wiley, 1232 pp., 2012.
- Shen, H., Chen, Z., Li, H., Qian, X., Qin, X., and Shi, W.: Gas-Particle Partitioning of Carbonyl Compounds in the Ambient Atmosphere, *Environmental Science & Technology*, 52, 10997-11006, 10.1021/acs.est.8b01882, 2018.
- Shen, J., Liu, X., Zhang, Y., Fangmeier, A., Goulding, K., and Zhang, F.: Atmospheric ammonia and particulate ammonium from agricultural sources in the North China Plain, *Atmospheric Environment*, 45, 5033-5041, 10.1016/j.atmosenv.2011.02.031, 2011.
- 360 Silvern, R. F., Jacob, D. J., Kim, P. S., Marais, E. A., Turner, J. R., Campuzano-Jost, P., and Jimenez, J. L.: Inconsistency of ammonium-sulfate aerosol ratios with thermodynamic models in the eastern US: a possible role of organic aerosol, *Atmos. Chem. Phys.*, 17, 5107-5118, 10.5194/acp-17-5107-2017, 2017.
- Stewart, W. M., Dibb, D. W., Johnston, A. E., and Smyth, T. J.: The Contribution of Commercial Fertilizer Nutrients to Food Production, *Agronomy Journal*, 97, 1-6, 10.2134/agronj2005.0001, 2005.
- 365 Sun, K., Tao, L., Miller, D. J., Pan, D., Golston, L. M., Zondlo, M. A., Griffin, R. J., Wallace, H. W., Leong, Y. J., Yang, M. M., Zhang, Y., Mauzerall, D. L., and Zhu, T.: Vehicle Emissions as an Important Urban Ammonia Source in the United States and China, *Environmental Science & Technology*, 10.1021/acs.est.6b02805, 2016.
- Sun, Y., Jiang, Q., Wang, Z., Fu, P., Li, J., Yang, T., and Yin, Y.: Investigation of the sources and evolution processes of severe haze pollution in Beijing in January 2013, *Journal of Geophysical Research: Atmospheres*, 119, 4380-4398, 10.1002/2014JD021641, 2014.
- 370 Tan, Y., Perri, M. J., Seitzinger, S. P., and Turpin, B. J.: Effects of Precursor Concentration and Acidic Sulfate in Aqueous Glyoxal-OH Radical Oxidation and Implications for Secondary Organic Aerosol, *Environmental Science & Technology*, 43, 8105-8112, 10.1021/es901742f, 2009.
- Turšič, J., Berner, A., Podkrajšek, B., and Grgič, I.: Influence of ammonia on sulfate formation under haze conditions, *Atmospheric Environment*, 38, 2789-2795, 10.1016/j.atmosenv.2004.02.036, 2004.
- 375 Wang, G., Zhang, R., Gomez, M. E., Yang, L., Levy Zamora, M., Hu, M., Lin, Y., Peng, J., Guo, S., Meng, J., Li, J., Cheng, C., Hu, T., Ren, Y., Wang, Y., Gao, J., Cao, J., An, Z., Zhou, W., Li, G., Wang, J., Tian, P., Marrero-Ortiz, W., Secret, J., Du, Z., Zheng, J., Shang, D., Zeng, L., Shao, M., Wang, W., Huang, Y., Wang, Y., Zhu, Y., Li, Y., Hu, J., Pan, B., Cai, L., Cheng, Y., Ji, Y., Zhang, F., Rosenfeld, D., Liss, P. S., Duce, R. A., Kolb, C. E., and Molina, M. J.: Persistent sulfate formation from London Fog to Chinese haze, *Proceedings of the National Academy of Sciences*, 113, 13630-13635, 10.1073/pnas.1616540113, 2016.
- 380 Wang, Q., Zhuang, G., Huang, K., Liu, T., Deng, C., Xu, J., Lin, Y., Guo, Z., Chen, Y., Fu, Q., Fu, J., and Chen, J.: Probing the severe haze pollution in three typical regions of China: Characteristics, sources and regional impacts, *Atmospheric Environment*, 120, 76-88, 10.1016/j.atmosenv.2015.08.076, 2015a.
- Wang, S., Nan, J., Shi, C., Fu, Q., Gao, S., Wang, D., Cui, H., Saiz-Lopez, A., and Zhou, B.: Atmospheric ammonia and its impacts on regional air quality over the megacity of Shanghai, China, *Scientific Reports*, 5, 15842, 10.1038/srep15842, 2015b.
- 385 Wang, Y., Zhang, Q. Q., He, K., Zhang, Q., and Chai, L.: Sulfate-nitrate-ammonium aerosols over China: response to 2000-2015 emission changes of sulfur dioxide, nitrogen oxides, and ammonia, *Atmos. Chem. Phys.*, 13, 2635-2652, 10.5194/acp-13-2635-2013, 2013.
- Warner, J. X., Dickerson, R. R., Wei, Z., Strow, L. L., Wang, Y., and Liang, Q.: Increased atmospheric ammonia over the world's major agricultural areas detected from space, *Geophysical Research Letters*, 44, 2875-2884, 10.1002/2016GL072305, 2017.



- Wei, L., Duan, J., Tan, J., Ma, Y., He, K., Wang, S., Huang, X., and Zhang, Y.: Gas-to-particle conversion of atmospheric ammonia and sampling artifacts of ammonium in spring of Beijing, *Science China Earth Sciences*, 58, 345-355, 10.1007/s11430-014-4986-1, 2015.
- 390 Wells, M., Choulaton, T. W., and Bower, K. N.: A modelling study of the interaction of ammonia with cloud, *Atmospheric Environment*, 32, 359-363, 10.1016/S1352-2310(97)00199-4, 1998.
- Wen, X., He, Z., and Zhang, Z.: Surveying and Evaluating of Land Environmental Quality and Monitoring of Basic Farmland Environmental Quality in Shanghai, *Shanghai Land & Resources*, 32, 8-13 [In Chinese], 2011.
- 395 Wu, Y., Gu, B., Erisman, J. W., Reis, S., Fang, Y., Lu, X., and Zhang, X.: PM<sub>2.5</sub> pollution is substantially affected by ammonia emissions in China, *Environmental Pollution*, 218, 86-94, 10.1016/j.envpol.2016.08.027, 2016.
- Wu, Z., Wang, Y., Tan, T., Zhu, Y., Li, M., Shang, D., Wang, H., Lu, K., Guo, S., Zeng, L., and Zhang, Y.: Aerosol liquid water driven by anthropogenic inorganic salts: Implying its key role in haze formation over the North China Plain, *Environmental Science & Technology Letters*, 5, 160-166, 10.1021/acs.estlett.8b00021, 2018.
- 400 Xu, J., Wang, Q., Deng, C., McNeill, V. F., Fankhauser, A., Wang, F., Zheng, X., Shen, J., Huang, K., and Zhuang, G.: Insights into the characteristics and sources of primary and secondary organic carbon: High time resolution observation in urban Shanghai, *Environmental Pollution*, 233, 1177-1187, 10.1016/j.envpol.2017.10.003, 2018.
- Xu, L., Guo, H., Weber, R. J., and Ng, N. L.: Chemical Characterization of Water-Soluble Organic Aerosol in Contrasting Rural and Urban Environments in the Southeastern United States, *Environmental Science & Technology*, 51, 78-88, 10.1021/acs.est.6b05002, 2017a.
- 405 Xu, W., Han, T., Du, W., Wang, Q., Chen, C., Zhao, J., Zhang, Y., Li, J., Fu, P., Wang, Z., Worsnop, D. R., and Sun, Y.: Effects of Aqueous-Phase and Photochemical Processing on Secondary Organic Aerosol Formation and Evolution in Beijing, China, *Environmental Science & Technology*, 51, 762-770, 10.1021/acs.est.6b04498, 2017b.
- Yang, X., and Fang, S.: Practices, perceptions, and implications of fertilizer use in East-Central China, *Ambio*, 44, 647-652, 10.1007/s13280-015-0639-7, 2015.
- 410 Yao, X., Yan Ling, T., Fang, M., and Chan, C. K.: Comparison of thermodynamic predictions for in situ pH in PM<sub>2.5</sub>, *Atmospheric Environment*, 40, 2835-2844, 10.1016/j.atmosenv.2006.01.006, 2006.
- Ye, X., Ma, Z., Zhang, J., Du, H., Chen, J., Chen, H., Yang, X., Gao, W., and Geng, F.: Important role of ammonia on haze formation in Shanghai, *Environmental Research Letters*, 6, 024019, 2011.
- Zhang, L., Chen, Y., Zhao, Y., Henze, D. K., Zhu, L., Song, Y., Paulot, F., Liu, X., Pan, Y., Lin, Y., and Huang, B.: Agricultural ammonia emissions in China: reconciling bottom-up and top-down estimates, *Atmos. Chem. Phys.*, 18, 339-355, 10.5194/acp-18-339-2018, 2018.
- 415 Zhang, R., Khalizov, A., Wang, L., Hu, M., and Xu, W.: Nucleation and growth of nanoparticles in the atmosphere, *Chemical Reviews*, 112, 1957-2011, 10.1021/cr2001756, 2011.
- Zhang, X., Wu, Y., Liu, X., Reis, S., Jin, J., Dragosits, U., Van Damme, M., Clarisse, L., Whitburn, S., Coheur, P.-F., and Gu, B.: Ammonia Emissions May Be Substantially Underestimated in China, *Environmental Science & Technology*, 51, 12089-12096, 10.1021/acs.est.7b02171, 2017.
- 420

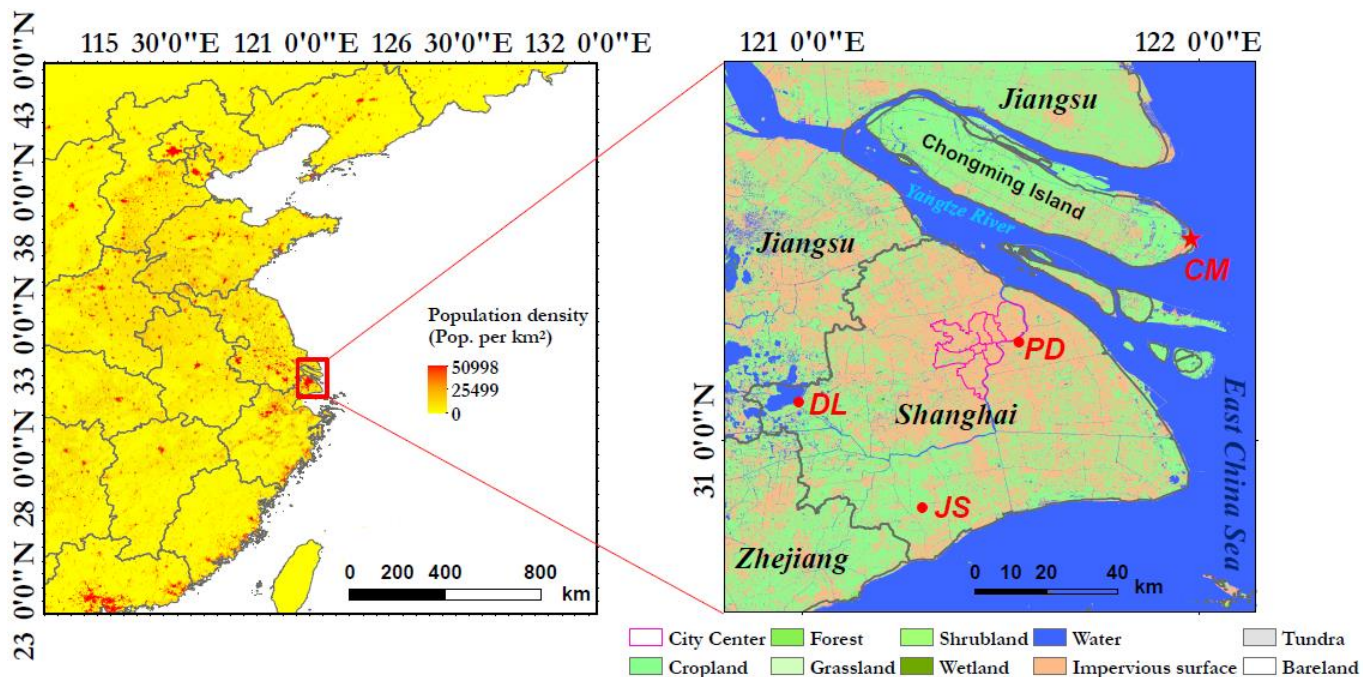
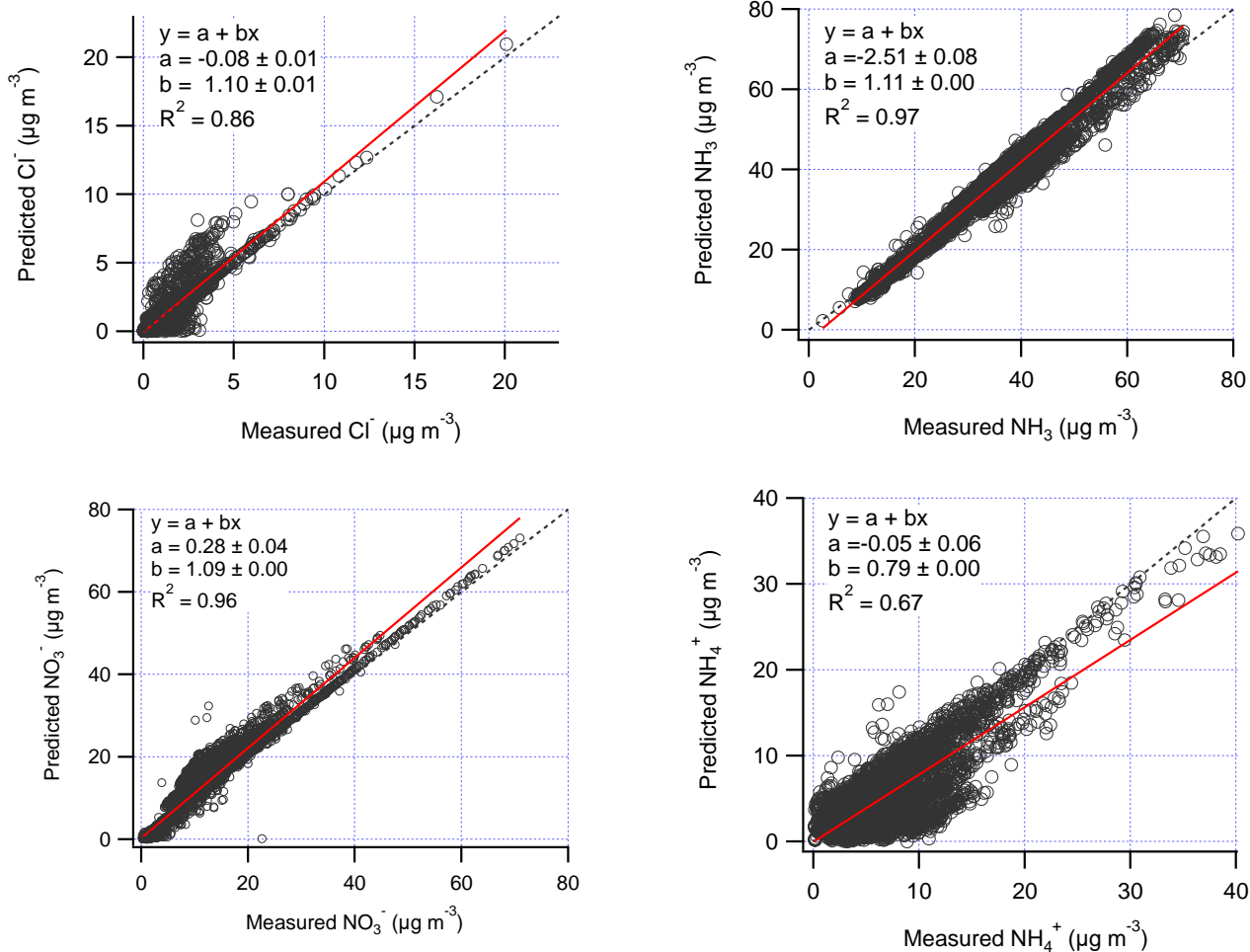
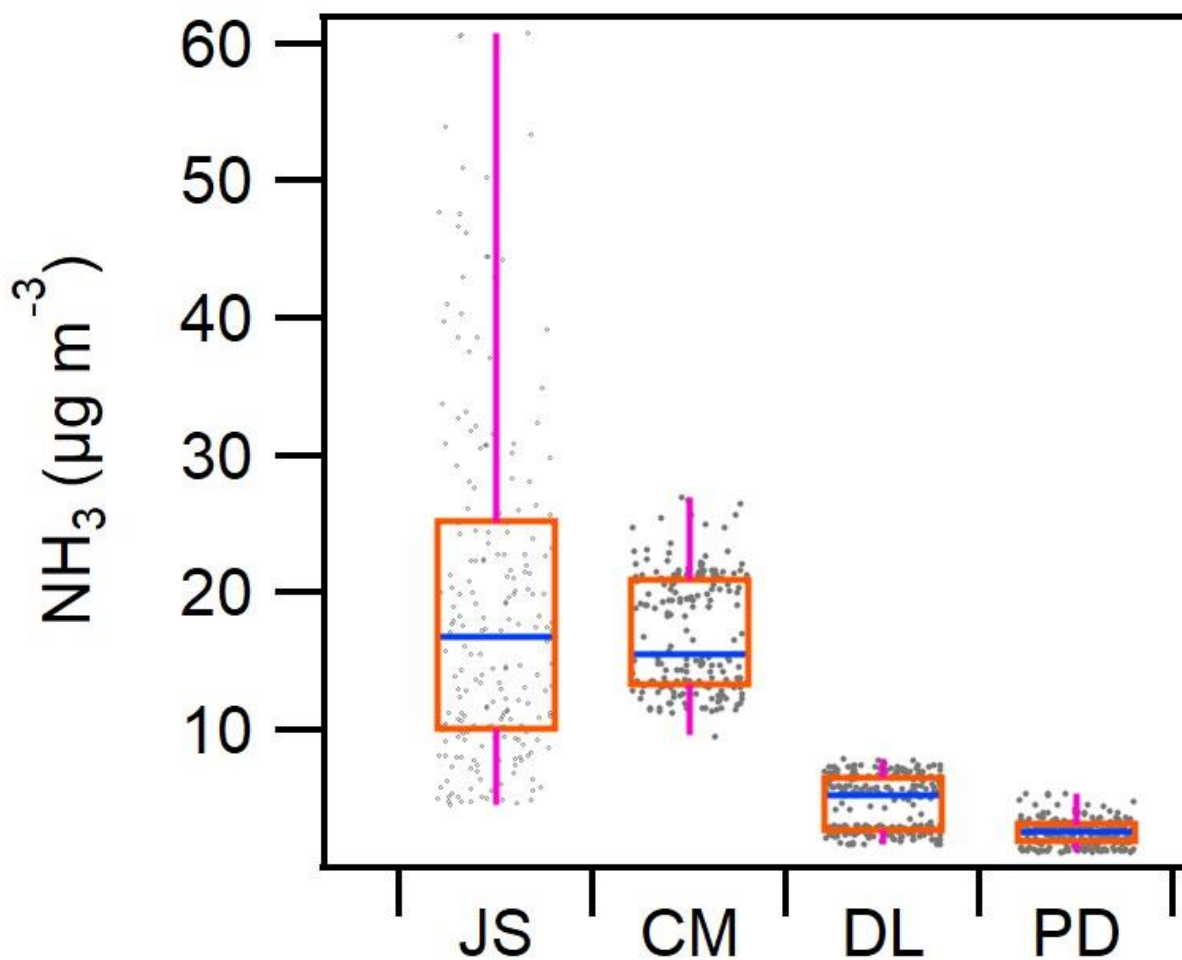


Figure 1: Location of the sampling site. Population density is color-coded in the left panel. The right panel shows the land cover in Shanghai (adapted from Peng et al.(2018)). CM (Chongming) is the sampling site on Chongming island. JS (Jinshan) represents the source emission from a dairy farm in rural Shanghai. DL (Dianshan Lake) represents a regional transport region in the Yangtze River Delta. PD (Pudong) represents the urban site.



430 **Figure 2: Comparison of predicted and measured Cl<sup>-</sup>, NO<sub>3</sub><sup>-</sup>, NH<sub>3</sub>, NH<sub>4</sub><sup>+</sup>. Orthogonal distance regression (ODR) fits with ±1σ are shown.**



**Figure 3:**  $\text{NH}_3$  at different sampling site over the same period (From Jan 18 to 27 of 2018). The locations of all sites are shown in Figure 1. Scattered dots indicate raw data points.

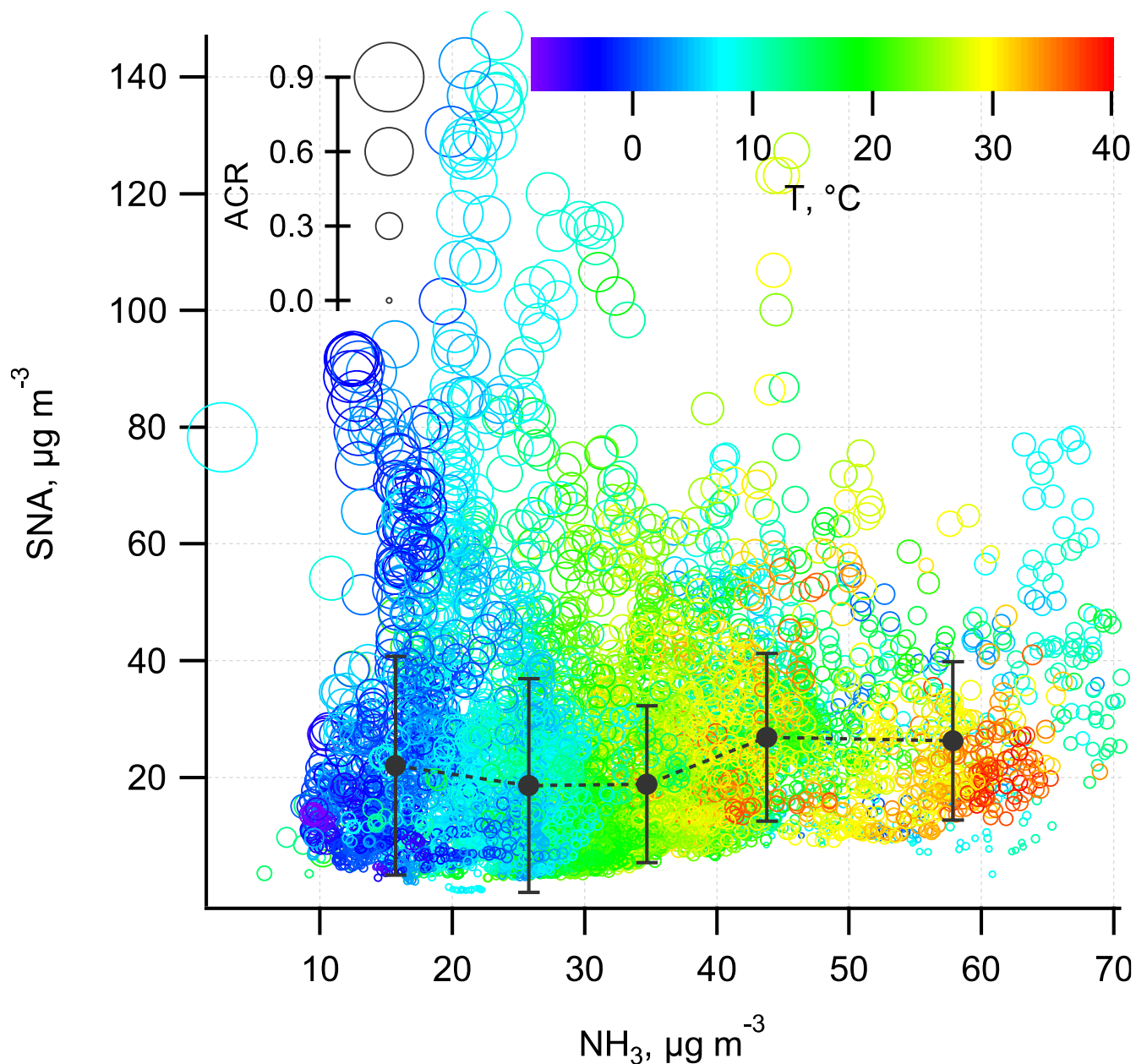
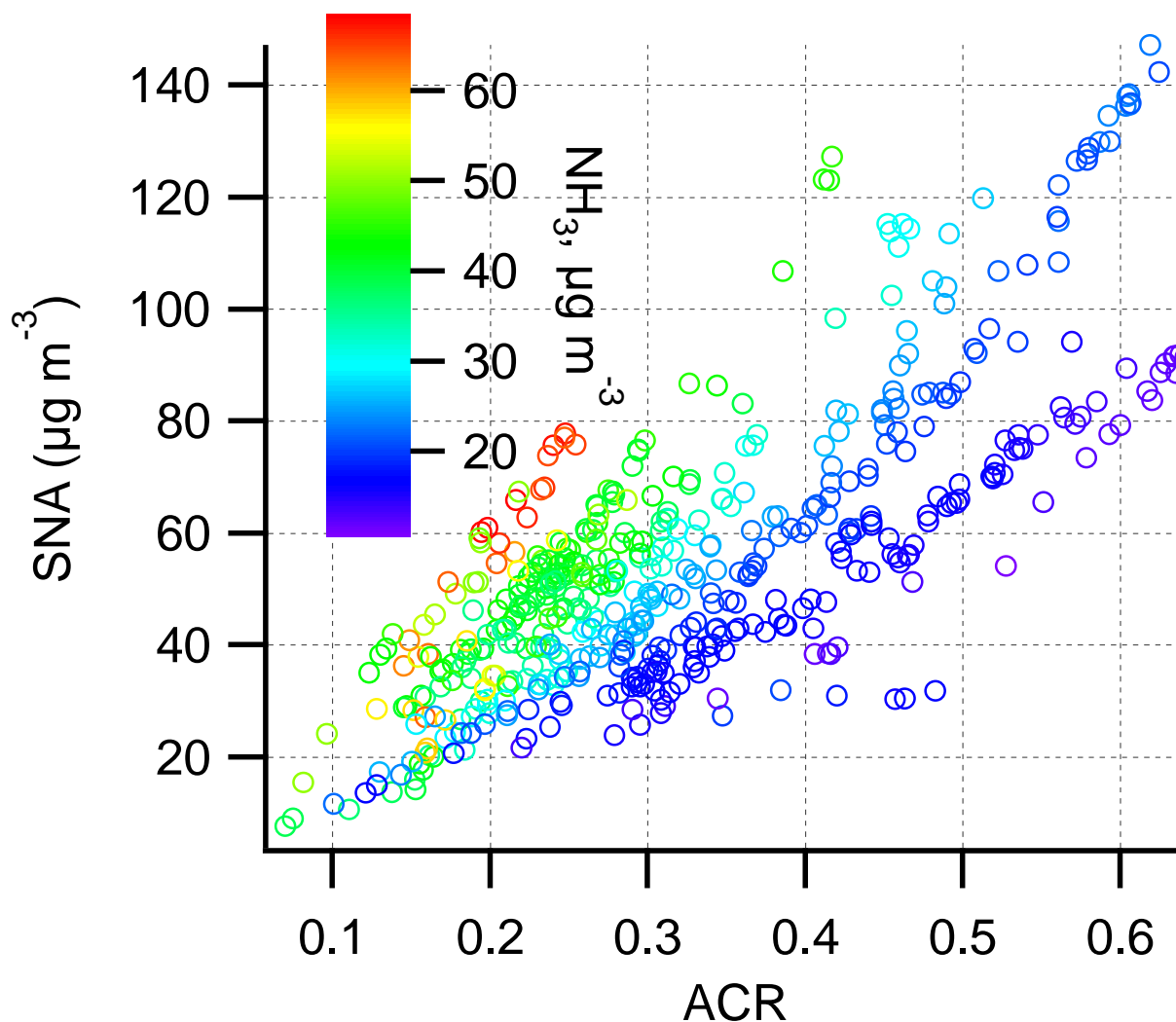


Figure 4: Secondary inorganic aerosol mass concentration in PM<sub>2.5</sub> (SNA refers to sulfate, nitrate, and ammonium) as a function of NH<sub>3</sub>. The sizes of the void circles are scaled to the ACR and colored by T. The SNA concentrations in black filled circles are binned and averaged according to the NH<sub>3</sub> mass concentration of each 10  $\mu\text{g m}^{-3}$ . Error bars represent one standard deviation ( $\pm 1\sigma$ ).

440



**Figure 5: SNA mass concentration in PM<sub>2.5</sub> as a function of ACR during the haze period. The circles are colored by the NH<sub>3</sub> mass concentration.**



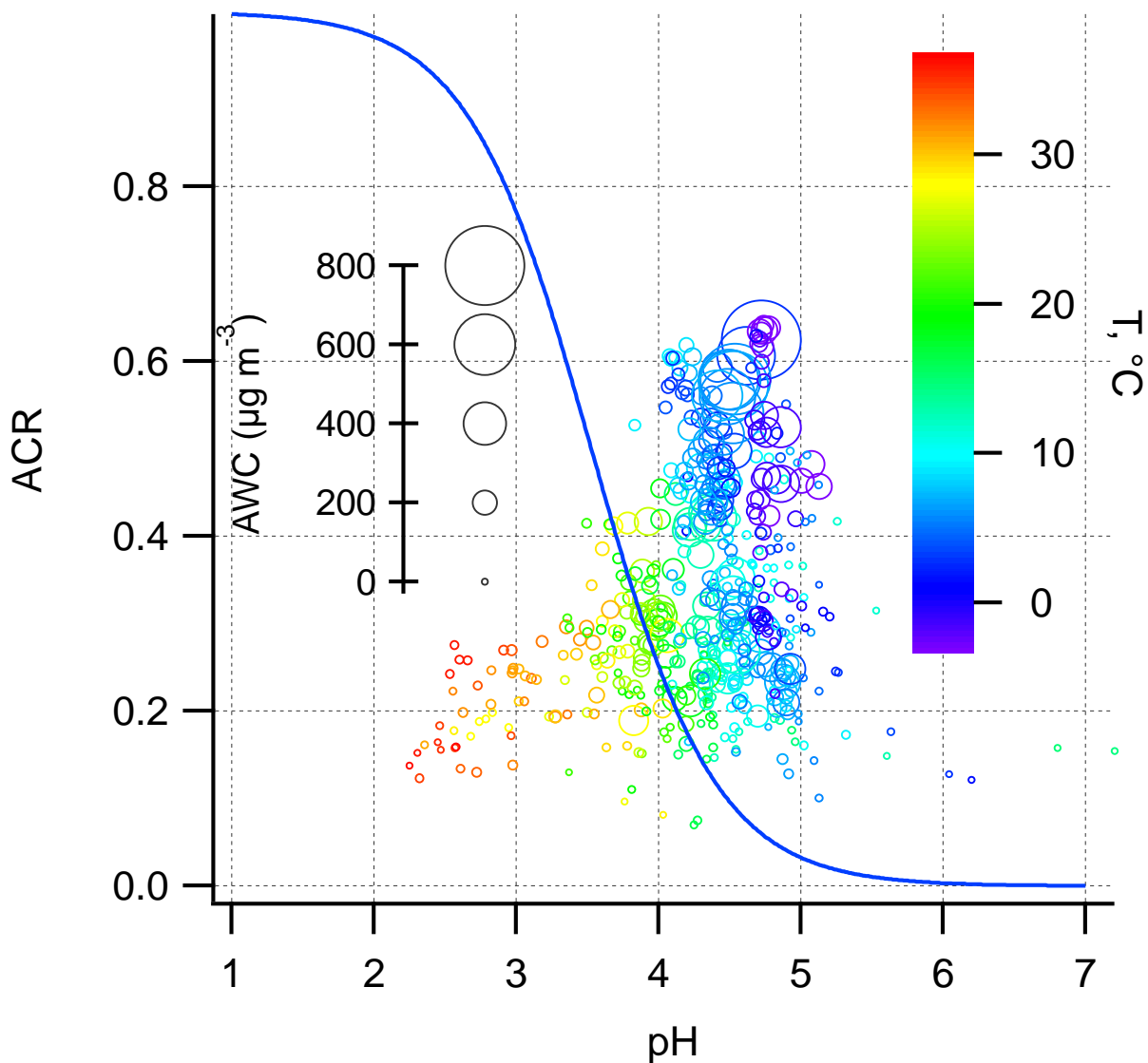
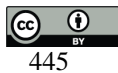


**Figure 6:** ACR as a function of pH during the haze period. The sizes of the void circles are scaled to AWC and colored by T. The blue curve was calculated based on the average T (10 °C), AWC (100  $\mu\text{g m}^{-3}$ ), and activity coefficients ratio of  $\frac{\gamma_{H^+}}{\gamma_{NH_4^+}}$  respectively. The average  $\frac{\gamma_{H^+}}{\gamma_{NH_4^+}}$  for the haze period is  $2.4 \pm 2.0 (\pm 1\sigma)$ .



450

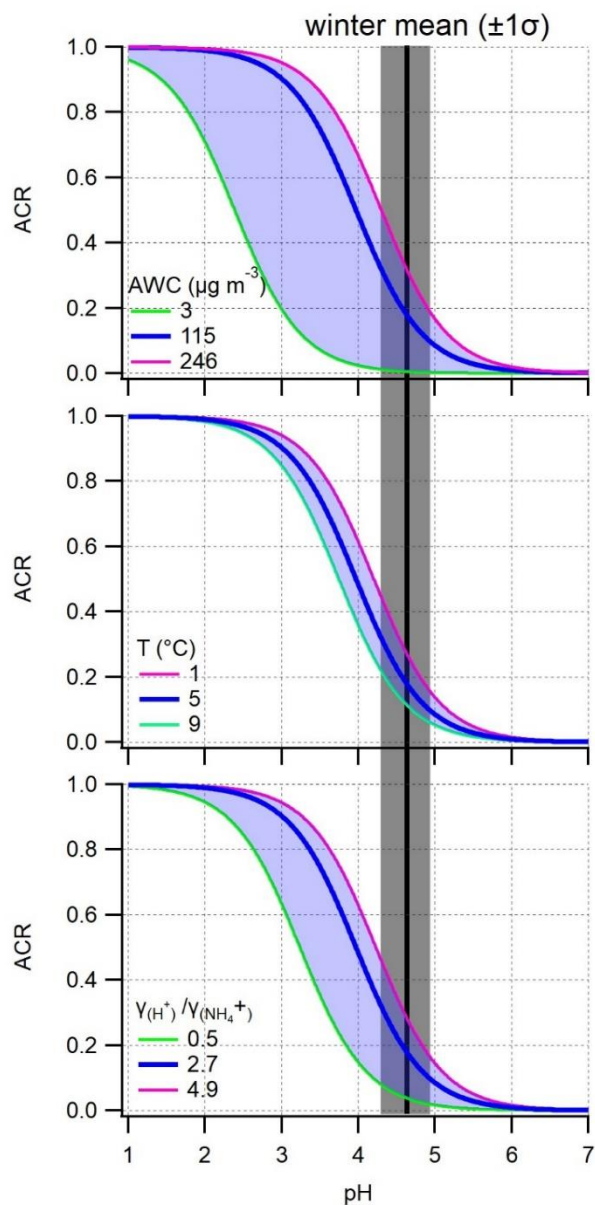


**Figure 7: ACR as a function of pH during the winter haze period. Other variables are held constant at the average value during the winter haze period, while varying only the AWC, T, activity coefficients ratio of  $\frac{\gamma_{H^+}}{\gamma_{NH_4^+}}$ , respectively.**

Shaded dark areas indicate the winter haze average pH together with one standard deviation ( $\pm 1\sigma$ ). Shaded blue areas represent the curve corresponding to average  $\pm 1\sigma$ , note that for AWC average -  $1\sigma$  yield a negative value, thus the minimum mass concentration ( $3 \mu\text{g m}^{-3}$ ) was used.

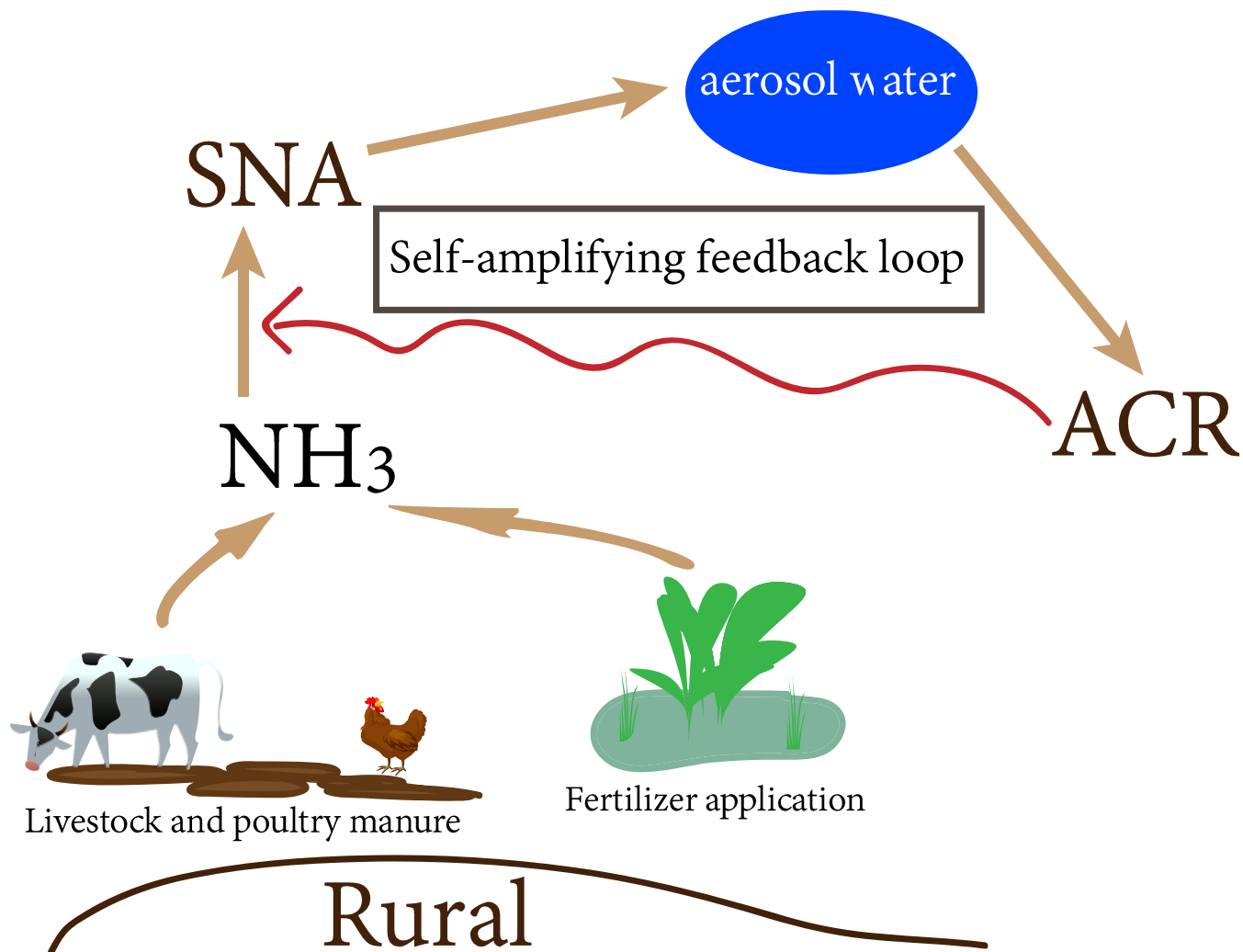


Figure 8: Schematic of self-amplifying feedback loop for SNA formation.

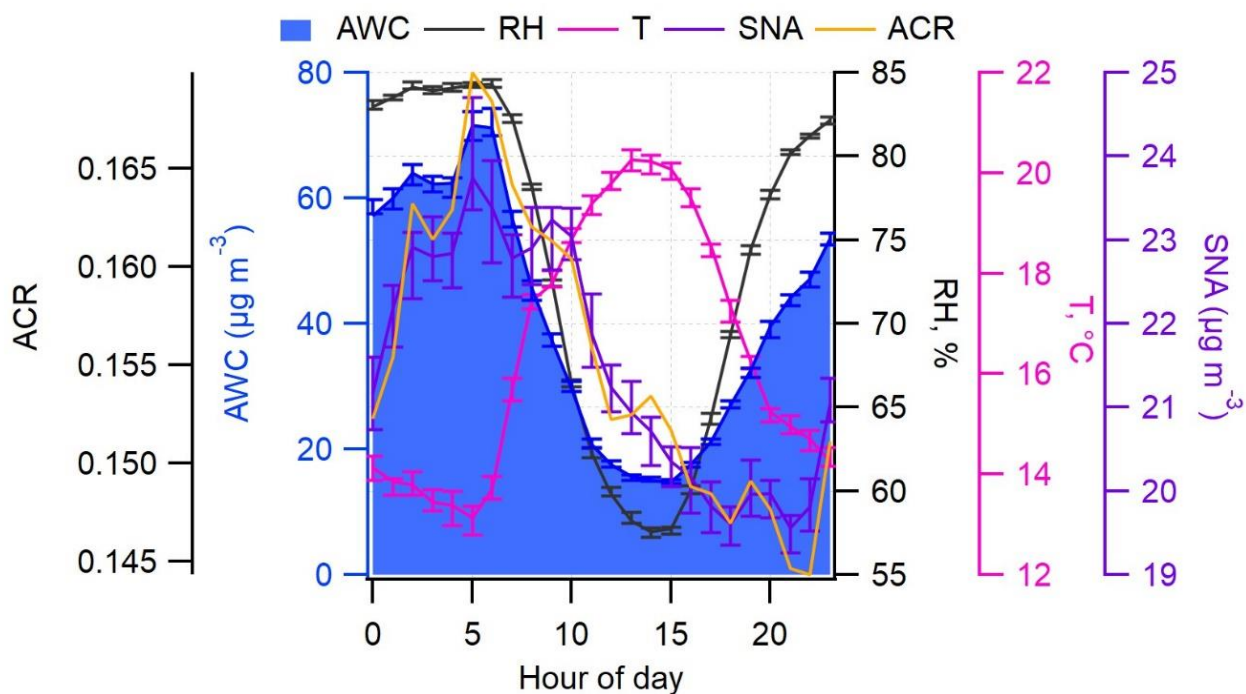


Figure 9: Annual mean diurnal pattern of ACR, AWC, SNA, T, and RH.



**Table 1:** The summer and winter average ( $\pm 1\sigma$ ) ACR, pH, T, activity coefficients ratio of  $\frac{\gamma_{H^+}}{\gamma_{NH_4^+}}$ , and  $NH_3$  ( $\mu g\ m^{-3}$ )

465 **during the haze period.**

	ACR	AWC	pH	$NH_3$	$\frac{\gamma_{H^+}}{\gamma_{NH_4^+}}$	T
summer	$0.2 \pm 0.1$	$79 \pm 73$	$3.4 \pm 0.5$	$40 \pm 8$	$1.8 \pm 1.7$	$29 \pm 5$
winter	$0.4 \pm 0.1$	$115 \pm 131$	$4.6 \pm 0.3$	$20 \pm 4$	$2.7 \pm 2.2$	$5 \pm 4$